ADVANCED THEORY AND SIMULATIONS
www.advtheorysimul.com

On the Molecular to Continuum Modeling of Fiber-Reinforced Composites

Ameya Rege and Sandeep P. Patil*

A multiscale approach to model fiber-reinforced composites, those that are characterized by an isotropic orientation of fibers, is presented. To this end, a bottom-up approach is used to formulate a hierarchical model. The primary basis for the mesoscopic description revolves around the assumption that the composite network consists of fibers resting on foundations of the native material matrix. Molecular dynamics (MD) simulations of such fibers on foundations are performed, and crucial material parameters, such as the stiffness of the particle matrix and Young's modulus of the fibers are evaluated. Subsequently, a micro-mechanical constitutive model is formulated, wherein fiber-reinforced composites are characterized by a homogeneous distribution and an isotropic orientation of fibers. The fibers are modeled as beams undergoing bending and stretching while resting on Winkler-type of elastic foundations. The 3D macroscopic network behavior is finally presented. As an example, the particle matrix used is a silica aerogel and the fibers are modeled as double-walled carbon nanotubes. In the proposed modeling approach, MD simulations are shown to provide a physical estimation of the micro-mechanical model parameters.

1. Introduction

There has been a steady rise in the literature of fiber-reinforced composites developed for a wide range of structural and engineering applications. Such reinforcement is typically introduced to enhance the load-bearing capacity of the materials while retaining the native properties of the matrix material. Fiber-reinforced composites can be generally classified into four categories: composites consisting of i) uni-directional fibers, ii) bi-directional fibers, iii) tri-directional fibers, and iv) randomly dispersed fibers. Uniaxial fiber-reinforced composites are the most well studied and applied ones as they exhibit significant strength in the direction of loading, considering the loading in a particularly given direction is critical while the loads in the other directions are of lesser importance to the application. Of growing interest are reports on the modeling of such composites. Most of the literature on micro-macro modeling of fiber-reinforced composites deals with those having a fixed orientation of fibers (uni-directional fibers or bi-directional fibers).

Studies on composites with dispersed fibers are rather scarce. In such cases, under deformation, the transmission of the load takes place from the matrix phase to fibers and vice versa. Micro-mechanical models of such fiber-reinforced composites with a random or isotropic orientation of fibers have been proposed based on mean-field homogenization procedures[1] and progressive debonding damage.[2] Moreover, Thomason[3] studied the influence of the fiber length, orientational distribution, and fiber concentration on the strength of the composite. On the other hand, reports on hierarchical modeling, for example, from an atomistic to continuum description, on such fiber-reinforced composites are relatively scarce. A review chapter on such a description was presented by Chandra.[4] In this regard, studies of carbon nanotube (CNT) reinforced composites have shown a presence. Odegard et al.[5] reported several types of model descriptions for single-walled carbon nanotube (SWCNT)-reinforced polymer composites. Fiber-reinforced silica aerogels have been of an academic as well as industrial interest in the past two decades. Parmenter and Milstein[6] first investigated the effect of fiber-reinforcement on silica aerogels. Meador et al.[7] showed that including up to 5% of carbon nanofibers in the silica aerogels resulted in a threefold increment in the compressive modulus while a fivefold increment in the tensile stress at break. Fiber-reinforcement of aerogels is seen as an effective method to harness the exclusive thermal and acoustic insulation features of aerogels with the mechanical strength and flexibility of fibers. An overview of the different reinforcing strategies applied to silica aerogels can be found in Maleki et al.[8] On the simulations front, Lu et al.[9] presented a two-level multiscale model of fiber-reinforced silica aerogels to capture the deformation under tension. The silica aerogels were modeled using a diffusion-limited

Dr. A. Rege
Department of Aerogels and Aerogel Composites
Institute of Materials Research
German Aerospace Center
Linder Höhe, 51147 Cologne, Germany
E-mail: ameya.rege@dlr.de
Dr. S. P. Patil
Institute of General Mechanics
RWTH Aachen University
Templergraben 64, 52062 Aachen, Germany

The ORCID identification number(s) for the author(s) of this article can be found under https://doi.org/10.1002/adts.201900211

DOI: 10.1002/adts.201900211

cluster-cluster aggregation (DLCA) algorithm, while the fibers were modeled in a finite element (FE) framework.

In this paper, a multiscale description of modeling the mechanical behavior of fiber-reinforced composites with an isotropic oriented and dispersed fibers is presented. As an example, fiber-reinforced silica aerogels are studied. However, the model approach may be applicable to many such composites having an isotropic orientation of fibers. The silica aerogel matrix is modeled based on our previous work.[10] Double-wall carbon nanotubes (DWCNTs) are modeled as short fibers dispersed in the aerogel matrix. To this end, first, molecular dynamics (MD) simulations are presented. Material parameters such as the Young's modulus of the DWCNTs and the stiffness in the aerogel matrix are determined. These are then used as input parameters in the continuum model. Here, the fibers are modeled as Euler–Bernoulli beams and these are considered to rest on the aerogel particle foundations. A 1D network model is described and then generalized to three dimensions using the microsphere approach.[11]

The paper is organized as follows. Section 2 elucidates the methods used in formulating the multiscale model. First, MD models are described. Second, a micro-mechanical model is formulated. Furthermore, its correlation with the MD model is illustrated. Section 3 displays the model results. MD results on silica aerogels, DWCNTs as well as the composite are first described. The results of the constitutive model are first verified with the MD results and last, a parameter study is presented. A conclusion and outlook are finally presented in Section 4.

2. Model Description

A hierarchical description of modeling fiber-reinforced composites is presented. First, to describe a micro-mechanically motivated continuum model, the following assumptions are made.

- The fibers are considered to behave as beams resting on elastic foundations of particles within the composite network.
- The fibers are considered to be isotropically oriented and homogeneously distributed through the material.

In order to evaluate the validity of the first assumption, an MD model within the same description framework is first analyzed. The required material parameters are derived from the MD model and used in the continuum model in the second step. The continuum model is also divided into two steps. A discrete mesoscopic 1D model is formulated. Directional averaging over a microsphere is then applied to obtain the 3D macroscopic response.

2.1. Molecular Dynamics Simulations

In this work, large-scale atomic/molecular massively parallel simulator (LAMMPS)[12] was used to perform MD simulations, and for visualization and analysis of the atomistic simulation data, OVITO[13] was used. For the atomistic modeling of silica aerogel, the Vashishta interatomic potential[14] was used. This potential is well suited for modeling of silica because it takes into account the pairwise interactions, the energy associated with the bonding angle and the orientation of three atoms. In our previous work,[10] the creation of the all-atom silica aerogel model has been discussed in detail. Here, only a brief description is presented.

Initially, to create bulk silica, the periodic boundary conditions were assigned in all three mutually perpendicular directions. The Velocity-Verlet algorithm was used with a time step size of 0.5 fs. The sample was heated to 7000 K, and subsequently, was quenched at constant volume and a constant number of atoms to 300 K at 5 K ps^{-1}. After the energy minimization and relaxation at atmospheric conditions (300 K and 1 bar), amorphous silica model was generated. The relaxed samples were instantaneously expanded in all three directions to the desired density ρ = 467, 628, 847 kg m^{-3}. The expanded samples were then heated to 3000 K for 50 ps, where MD systems were given the opportunity to overcome energetic barriers and to find the best conformations. Finally, the nanoporous silica aerogel was formed when the sample is further brought back to the atmospheric conditions.

In this work, for MD simulations of CNTs, the short-range interactions between the C–C atoms were defined by Brenner's second-generation reactive empirical bond-order (or REBO) force field,[15] while the van der Waals force (or Lennard–Jones potential) was adopted to describe the long-range interactions between the carbon atoms.

In the simulation systems, armchair CNTs were modeled on the silica aerogels. Therefore, it is essential to define the interatomic potential between Si, O, and C atoms. As discussed earlier, for the silica atoms[14] and the C–C atoms,[15] interactions have been defined with well-known interatomic potentials. For the Si–C and O–C interactions, we used the parameters proposed by Rappé et al.,[16] which were based primarily on the short-range van der Waals potential.[17] The parameters ϵ and σ were set as 8.909 meV and 3.326 Å, respectively, for Si–C interaction, and 3.442 meV and 3.001 Å, respectively, for O–C interaction.[18] In our previous work,[19] we used the parameters as mentioned earlier to perform nanoindentation tests on single- and multilayered graphene-reinforced silica aerogel nanocomposites.

The main focus of this work was to study the compressive resistance of the matrix due to the bending of reinforcing fibers. An impression of the composite formed of randomly dispersed fibers within the matrix is illustrated in **Figure 1**a. In accordance with the assumptions listed above, the interaction between the discrete fibers and the underlying particle foundations is investigated. Here, we modeled the double-walled carbon nanotube (DWCNT) as a reinforcement material. The DWCNT model has 11 480 atoms with (20,20) outer CNT and (15,15) inner CNT. The dimensions of the matrix model of silica aerogel foundation are $15 \times 15 \times 2.8$ nm^3, which is at the bottom and DWCNT model is on the top. Figure 1b,c show the undeformed and deformed configurations, respectively. After the whole MD system has been set up, the Maxwell–Boltzmann distribution was used to assign the initial velocities and then followed by energy minimization.[20] Subsequently, every MD simulation system was equilibrated at atmospheric conditions for 100 ps using the NVT ensemble to reach a steady state. Finally, the bending of reinforcement simulations was carried out with the NVE (constant volume constant internal energy) ensemble.

The silica aerogels having densities 467, 628, and 847 kg m^{-3} were considered. In order to examine the length influence of reinforcement, three different lengths of 20, 25, and 30 nm of DWCNTs were modeled. During the deformation of this

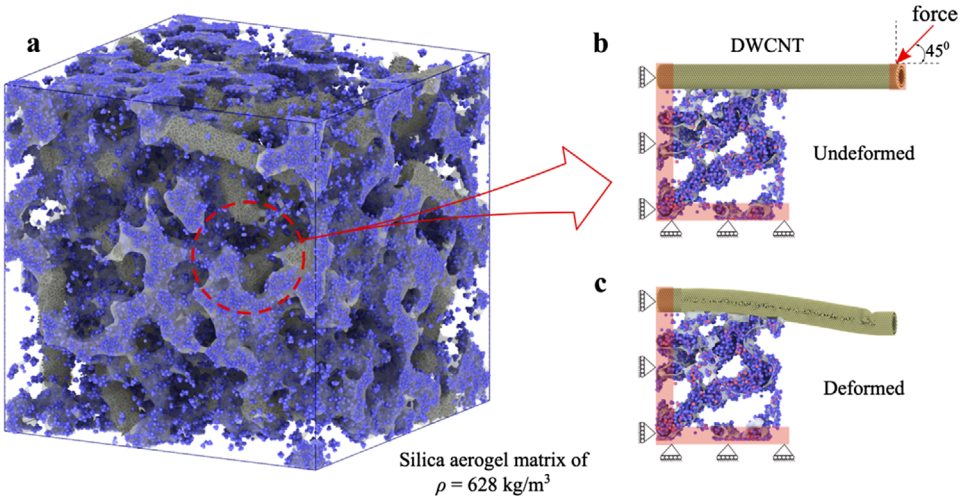

Figure 1. Illustration of a) a fiber-reinforced silica aerogel. Schematic representation of the representative element of a fiber resting on a foundation of aerogel particles, b) in the undeformed state, and c) in the deformed state.

combined model, the bottom and left portions of 1.6 nm were fully constrained in all directions as shown in Figure 1b. The force was applied to the free end of both tubes of the DWCNT (see the highlighted part at the end of the DWCNT in Figure 1b).

The elastic modulus (E) of the DWCNT model can be determined from the potential energy–strain relationship during the tension process. Mathematically, E is expressed as

$$E = \frac{1}{V_0}\frac{d^2U}{d\epsilon^2} \tag{1}$$

where U denotes the strain energy stored in the carbon atoms that are subjected to axial loading, ϵ is a strain, which is defined as the ratio of change in length to the original length, and V_0 is the original volume of the DWCNT. V_0 is calculated using the formula $V_0 = L_0\ A_c$, where L_0 is the original length, and A_c is the initial cross-sectional area of the DWCNT. A_c is defined as $A_c = \pi dh$, where h is the thickness of the nanotube layer.

2.2. Micro-Mechanical Modeling

The model Ansatz is as described above and illustrated in Figure 1b. Within the framework of a micro-mechanical approach, the fibers are modeled as Euler–Bernoulli beams. The particle foundation is considered to be of the Winkler type. Kanninen[21] described the mathematical formulation of Euler–Bernoulli beams on Winkler foundations. These are applied, and the total strain energy of one fiber resting on a foundation of particles is decomposed into the bending component and the tension one. First, the bending strain energy for a fiber resting on an elastic foundation of matrix particles can be expressed as[21]

$$\psi_{ben} = 6EI\eta^3(1-\lambda)^2l^2\sin^2\varphi\cos^2\varphi \times \left[2\eta^3l^3 + 6\eta^2l^2\left(\frac{\sinh\eta s\cosh\eta s + \sin\eta s\cos\eta s}{\sinh^2\eta s - \sin^2\eta s}\right) + 6\eta l\left(\frac{\sinh^2\eta s + \sin^2\eta s}{\sinh^2\eta s - \sin^2\eta s}\right) + 3\left(\frac{\sinh\eta s\cosh\eta s - \sin\eta s\cos\eta s}{\sinh^2\eta s - \sin^2\eta s}\right)\right]^{-1} \tag{2}$$

where E and I denote the Young's modulus and the area moment of inertia of the fiber, respectively. Furthermore, l and φ represent the free length of the fiber and angle of orientation of the fiber, respectively. Last, λ and s denote the applied micro-stretch and the length of the foundation resting under the fiber, respectively. Furthermore

$$\eta^4 = \frac{k}{4EI} \tag{3}$$

where k identifies the initial stiffness in the elastic foundation. This corresponds to the stiffness of the silica aerogel matrix, for our case. The numerical value of k is evaluated in by means of MD simulations and will be discussed in the next section.

Furthermore, the particles resting below are considered to play no role for axial tension or compression of the fiber. Thus, the frictional effects between the fibers and particles are neglected. Thus, the tension strain energy can be solely expressed as formulated in Rege and Itskov[22]

$$\psi_{axl} = \frac{EA\,(l+s)\,(1-\lambda)^2\sin^4\varphi}{2} \tag{4}$$

where A is the cross section area of the fiber. The total strain energy of a fiber on an elastic foundation of particles is then given by

$$\psi_{tot} = \psi_{ben} + \psi_{axl} \tag{5}$$

Among others, the above-defined strain energy function depends on the length of the fiber, which is not constant through the network. To this end, a Gaussian distribution function is considered over the lengths of fibers l_{min} and l_{max} in order to account

for its variation. Variations in other parameters, if any, could also be incorporated in this step. The 1D network energy is then expressed as

$$\psi^d = \int_{l_{\min}}^{l_{max}} \psi_{\text{tot}} N_f p(l) dl \tag{6}$$

where N_f represents the total number of initial fibers in the network and $p(l)$ denotes the probability distribution function and corresponds to the Gaussian distribution function. In the case of the possession of a priori knowledge regarding the distribution of fiber lengths, the respective distribution or a mathematical fit to it can be used here. The 1D model is generalized to 3D by means of numerical integration over the unit sphere. The algorithm by Bažant and Oh[23] is used. Accordingly, the 3D network strain energy can be represented as

$$\Psi = \frac{1}{A} \int_S \psi^d dS \approx \sum_{i=1}^{21} \omega_i \psi^{d_i} \tag{7}$$

It should be noted that affine deformation mapping is considered. Accordingly, the microscopic stretches follow the macroscopic deformation gradient. The constitutive equation is finally presented in the form of the first Piola–Kirchhoff stress tensor as

$$\mathbf{P} = \frac{\partial \Psi}{\partial \mathbf{F}} = \frac{\partial \Psi}{\partial \lambda^{d_i}} \frac{\partial \lambda^{d_i}}{\partial \mathbf{F}} \tag{8}$$

where $\mathbf{F}$ is the macroscopic deformation gradient. The above-defined constitutive equation can be applied to describe the macroscopic mechanical behavior of such fiber-reinforced composites that fit the framework of the proposed model.

3. Results

First, the results from MD simulations are analyzed and then, based on those, the results of the meso- to macro-scale model are interpreted. One of the essential unknown parameters in our model is the stiffness in the elastic foundation k, which is within the strain energy function of the mesoscopic model. To obtain this parameter, uniaxial compression tests were carried on the silica aerogel models using MD simulations. **Figure 2** shows the resulting force–displacement curves for three different densities of the silica aerogel models. Within the small deformation regime, the slope of the force-displacement curve gives the stiffness of the material. The initial slope of the curve in Figure 2 is accordingly considered to quantify the continuum model parameter k.

The Young's modulus of the DWCNT is evaluated as described in the previous section. The thickness h is taken to be 0.34 nm.[24] The elastic modulus of DWCNT was evaluated as 814.5 GPa (see **Figure 3**). This is in close agreement with the Young's modulus reported in the work of Demczyk et al.[25] Furthermore, fiber on an elastic foundation and specifically the corresponding application of the Euler–Bernoulli beam theory are assumptions used in our model. These are verified by means of MD simulations to analyze if the application of the beam theory is valid for our cases.

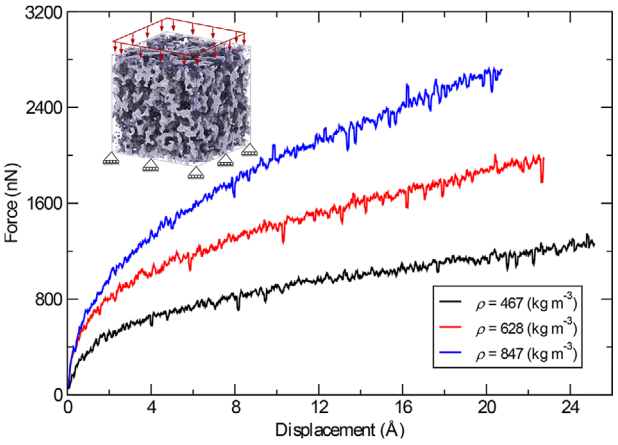

Figure 2. Force versus displacement curves for silica aerogels, compressed up to 5% strain. The slope of the curve gives the stiffness in the elastic foundation.

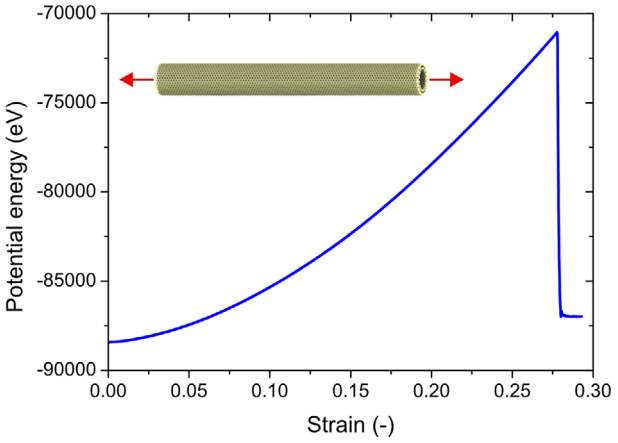

Figure 3. Illustration of tensile study on DWCNTs. Potential energy versus strain response of DWCNT in order to evaluate the Young's modulus.

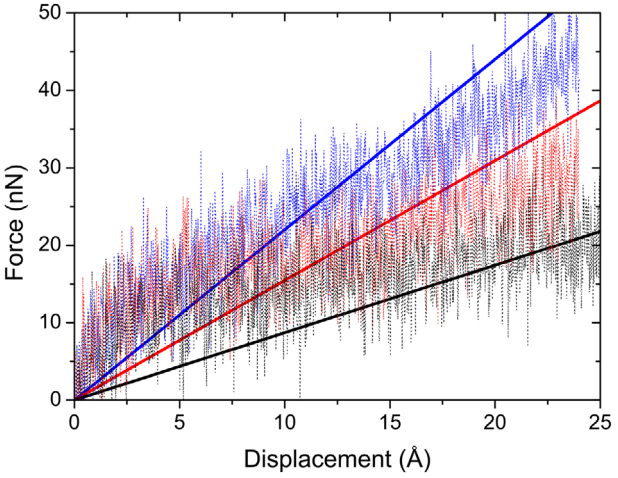

Figure 4. Force versus displacement curves of the fiber deflection on the foundation of aerogel particles: a comparison of the MD model (dotted lines) versus the continuum model (solid lines). The colors correspond to: blue: 30 nm CNT over a 15 nm aerogel foundation, red: 25 nm CNT over a 15 nm aerogel foundation, black: 20 nm CNT over a 15 nm aerogel foundation.

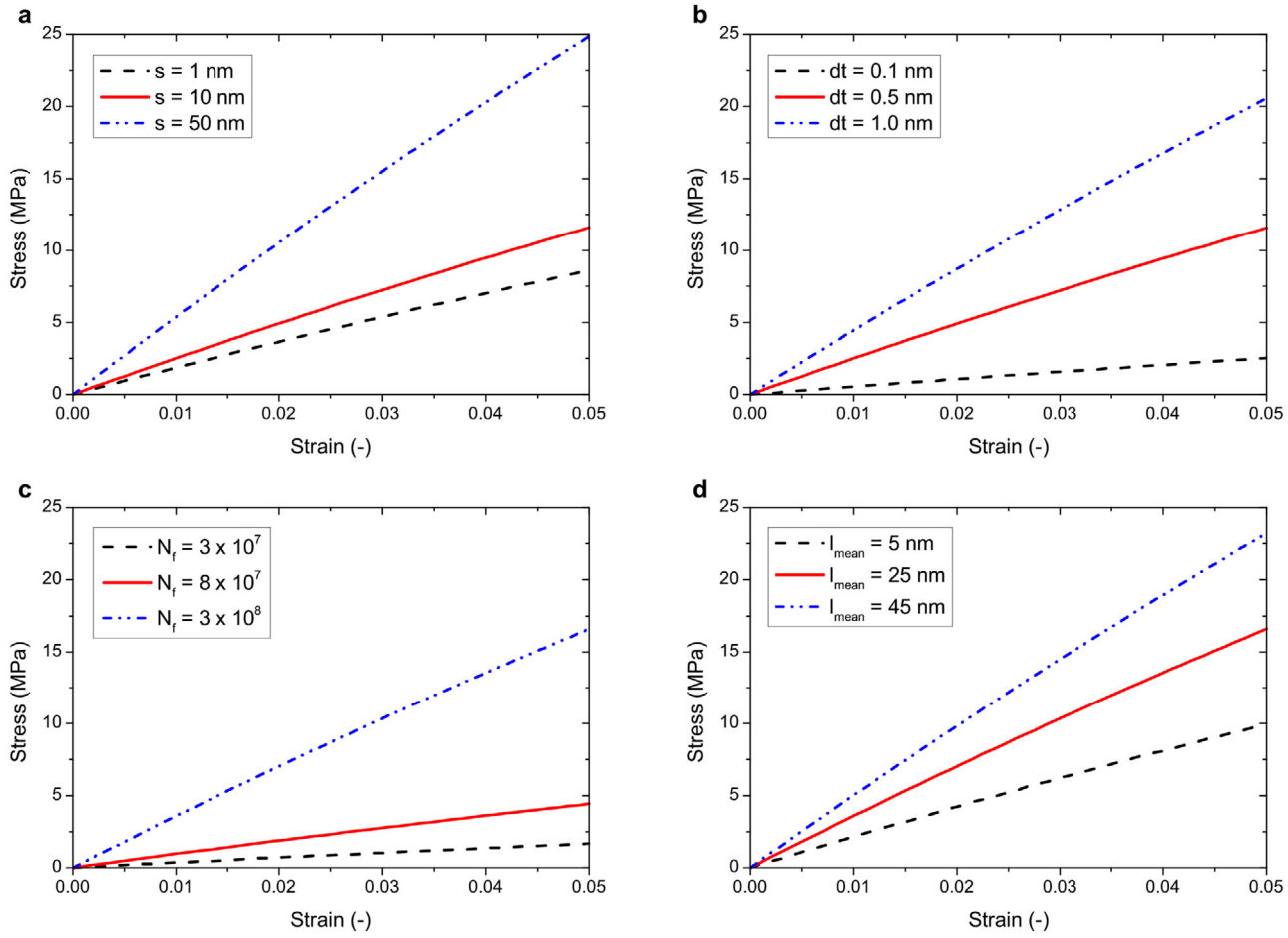

Figure 5. Model parameter sensitivity analysis. a) Variation in the extent of foundation *s*, b) variation in the CNT wall thickness $d_t = d_o - d_i$, c) variation in the number of fibers N_f, d) variation in the mean fiber length l_{mean}.

To verify the applicability of Equation (2) to CNT-reinforced silica aerogels, the force–displacement curves from the meso-model are verified against those generated from MD simulations. The results seem to be in agreement with each other (see **Figure 4**). There is much noise in the MD curves, and the overall response is also slightly nonlinear, especially with an initial steeper slope. On the other hand, the continuum model shows a linear response as expected. However, it must be noted that despite the fact that the model Ansatz is highly idealized, and most importantly, solely based on the computed parameters from MD calculations, the results of the beam theory are in bounds with the results from the MD data. Although it looks straightforward, this is a very important result, because it proves the applicability of our assumption: CNTs are modeled as beams and the underlying silica aerogel matrix is modeled as a Winkler-type of elastic foundation. Additionally, the MD contour plots of the DWCNTs on silica aerogel foundations, for two different load-application cases, are illustrated in Figures S1 and S2, Supporting Information. Moreover, the bending analysis of DWCNTs, with and without the foundation of a silica aerogel matrix, is provided in Figures S3 and S4, Supporting Information.

Upon validation of the discrete micro-model, the 3D continuum network response can be obtained by simulating the proposed network constitutive model. It contains the following material parameters, as listed in **Table 1**.

Table 1. Description of material parameters.

Parameter	Description
l_{min}, l_{max}	Minimum and maximum length of fibers
d_o, d_i	Outer and inner fiber diameter
E	Elasticity modulus of the fiber
k	Stiffness in the elastic foundation
N_f	Initial number of fibers in the network

Among these, the first four parameters, l_{min}, l_{max}, d_o and d_i, can be directly obtained from the product details based on the synthesis parameters. The next two parameters, E and k are typically unknown quantities and have been evaluated using MD simulations as described earlier. Finally, N_f, if known, can establish this model as one that could be developed into a predictive model for characterizing fiber-reinforced composites. All parameters in this model are physically motivated and can be either obtained via experimental synthesis parameters or by means of lower length scale simulation (MD, in this case) methods. Thus, the proposed

model is a true hierarchical multiscale or multi-level model involving molecular-micro-macro length scales while also incorporating atomistic and continuum modeling tools.

Figure 5 presents the sensitivity analysis of different model parameters on the macroscopic mechanical behavior. First, the extent of the particle foundation *s* is investigated in Figure 5a. It can be observed that increasing the extent of the foundation results in the stiffening of the bulk material response. Thus, higher this particle concentration under the fibers, stiffer is the response. This agrees well with the conclusion of Parmenter and Milstein[6] for higher particle concentration for a given fiber density. Next, the influence of increasing the thickness of the CNT wall is investigated (see Figure 5b). As can be expected, the thicker the fiber wall, the stiffer the bulk behavior. Next, the initial fiber content in the virgin matrix is varied, which depends on the user input during the synthesis process. Figure 5c shows that increasing the number of fibers N_f demonstrates a stiffer network response. This agrees well with the results of Thomason.[3] Last, the influence of the mean fiber length on the network behavior is studied in Figure 5d. The closer the mean of the probability density function to the minimum fiber length, the softer is the bulk material response for a given number of fibers within the matrix.

The presented model approach shows its ability to describe the macroscopic mechanical behavior of a fiber-reinforced composite based on a micro-mechanical Ansatz, which is reinforced with molecular dynamics simulation results. This approach could be applied to any such composite having a random fiber distribution. Although the current model shows very good predictive capabilities, it is also important to note its limitations. In its current form, it can only be applied to composites undergoing small-strain deformation. No damage mechanisms have yet been incorporated to account for inelastic effects in the network. Also, since the model uses a linear foundation, flexible matrices that undergo large deformations cannot be described using the proposed equations. On comparing with standard models such as the Neo–Hookean, the presented model is quite limited to capturing the mechanical response only under small deformations. However, the model is physically motivated and all parameters in the model have a direct correlation to the microstructural parameters. This opens the possibilities of such modeling approaches to be used for reverse engineering of composites based on the results of the numerical simulations. Furthermore, the presented strain energy equation is based on the standard Euler–Bernoulli beam theory. The equation could be modified to elucidate large deflections of such beams using nonlinear theories describing an elastic curve. Such extended beam theories have been used to describe the nonlinear behavior of fibers (see Rege et al.[26]). In this way and by incorporating damage criteria, the presented model approach is extendable for describing nonlinear inelastic deformations as well as to explore stress-softening effects resulting in deformation-induced anisotropy.

4. Conclusion

In this paper, a new hierarchical approach toward the multiscale description of fiber-reinforced composites is presented. The nanoscale properties of the fibers and the underlying matrix material are first simulated and evaluated using molecular dynamics simulations. The obtained parameters are further used as inputs to a continuum description of the model. Here, fibers are modeled as beams resting on a foundation of the matrix material. As only the small deformation behavior is investigated, the standard Euler–Bernoulli beam theory is shown to suffice to characterize the deformation of fibers. The discrete fiber-on-foundation model is validated against the molecular dynamics simulation data. The model consists of six micro-mechanically motivated material parameters. All of them are shown to be either obtained from experimental synthesis data and/or can be obtained from molecular simulations. Due to this reason, the model shows the capability to be further developed into a predictive model that can be used for reverse engineering of such fiber-reinforced composites to achieve desired tailored application-oriented behavior.

Supporting Information

Supporting Information is available from the Wiley Online Library or from the author.

Conflict of Interest

The authors declare no conflict of interest.

Keywords

carbon nanotubes, fiber-reinforced composites, multiscale models, silica aerogels

Received: October 22, 2019
Revised: January 10, 2020
Published online:

[1] I. Doghri, L. Tinel, *Int. J. Plast.* **2005**, *21*, 1919.
[2] F. Zaïri, M. Naït-Abdelaziz, J. M. Gloaguen, A. Bouaziz, J. M. Lefebvre, *Int. J. Solids Struct.* **2008**, *45*, 5220.
[3] J. L. Thomason, *Composites, Part A* **2008**, *39*, 1618.
[4] N. Chandra, in *Multiscale Modeling and Simulation of Composite Materials and Structures* (Eds: Y. W. Kwon, D. H. Allen, R. Talreja), Springer, Boston, MA **2008**, p. 579.
[5] G. M. Odegard, R. B. Pipes, P. Hubert, *Compos. Sci. Technol.* **2004**, *64*, 1011.
[6] K. E. Parmenter, F. Milstein, *J. Non-Cryst. Solids* **1998**, *223*, 179.
[7] M. A. B. Meador, S. L. Vivod, L. McCorkle, D. Quade, R. M. Sullivan, L. J. Ghosn, N. Clark, L. A. Capadona, *J. Mater. Chem.* **2008**, *18*, 1843.
[8] H. Maleki, L. Durães, A. Portugal, *J. Non-Cryst. Solids* **2014**, *385*, 55.
[9] Z. Lu, Z. Yuan, Q. Liu, Z. Hu, F. Xie, M. Zhu, *Mater. Sci. Eng., A* **2015**, *625*, 278.
[10] S. P. Patil, A. Rege, Sagardas, M. Itskov, B. Markert, *J. Phys. Chem. B* **2017**, *121*, 5660.
[11] C. Miehe, S. Göktepe, F. Lulei, *J. Mech. Phys. Solids* **2004**, *52*, 2617.
[12] S. Plimpton, *J. Comput. Phys.* **1995**, *117*, 1.
[13] A. Stukowski, *Modell. Simul. Mater. Sci. Eng.* **2009**, *18*, 015012.
[14] a) P. Vashishta, R. K. Kalia, A. Nakano, W. Li, I. Ebbsjö, in *Amorphous Insulators and Semiconductors* (Eds: M. F. Thorpe, M. I. Mitkova),

Kluwer, Dordrecht, The Netherlands **1996**, p. 151; b) P. Vashishta, R. K. Kalia, J. P. Rino, I. Ebbsjö, *Phys. Rev. B* **1990**, *41*, 12197.
[15] S. J. Stuart, A. B. Tutein, J. A. Harrison, *J. Chem. Phys.* **2000**, *112*, 6472.
[16] A. K. Rappé, C. J. Casewit, K. Colwell, W. A. Goddard III, W. M. Skiff, *J. Am. Chem. Soc.* **1992**, *114*, 10024.
[17] J. Xiao, S. Dunham, P. Liu, Y. Zhang, C. Kocabas, L. Moh, Y. Huang, K.-C. Hwang, C. Lu, W. Huang, *Nano Lett.* **2009**, *9*, 4311.
[18] Z. -Y. Ong, E. Pop, *Phys. Rev. B* **2010**, *81*, 155408.
[19] S. Patil, *Molecules* **2019**, *24*, 1336.
[20] J. Haile, I. Johnston, A. J. Mallinckrodt, S. McKay, *Comput. Phys.* **1993**, *7*, 625.
[21] M. F. Kanninen, *Int. J. Fract.* **1973**, *9*, 83.
[22] A. Rege, M. Itskov, *Acta Mech.* **2018**, *229*, 585.
[23] Z. P. Bažant, B. H. Oh, *J. Appl. Math. Mech.* **1986**, *66*, 37.
[24] Y. Huang, J. Wu, K.-C. Hwang, *Phys. Rev. B* **2006**, *74*, 245413.
[25] B. G. Demczyk, Y. M. Wang, J. Cumings, M. Hetman, W. Han, A. Zettl, R. Ritchie, *Mater. Sci. Eng., A* **2002**, *334*, 173.
[26] a) A. Rege, M. Schestakow, I. Karadagli, L. Ratke, M. Itskov, *Soft Matter* **2016**, *12*, 7079; b) A. Rege, I. Preibisch, M. Schestakow, K. Ganesan, P. Gurikov, B. Milow, I. Smirnova, M. Itskov, *Materials* **2018**, *11*, 1670.